Diabetes, Metabolic Syndrome and Obesity: Targets and Therapy Dovepress
open access to scientific and medical research

Open Access Full Text Article

ORIGINAL RESEARCH

Photobiomodulation at 830 nm Stimulates Migration, Survival and Proliferation of Fibroblast Cells

Olajumoke Arinola Oyebode, Nicolette Nadene Houreld

Laser Research Centre, Faculty of Health Sciences, University of Johannesburg, Doornfontein, Gauteng, South Africa

Correspondence: Olajumoke Arinola Oyebode, Laser Research Centre, Faculty of Health Sciences, University of Johannesburg, Doornfontein, Gauteng, South Africa, Tel + 27781519058, Email daramzjay09@gmail.com

Purpose: Photobiomodulation (PBM) promotes diabetic wound healing by favoring cell survival and proliferation. This study aimed to investigate the potential of PBM in stimulating cellular migration, viability, and proliferation using the transforming growth factor-β1 (TGF-β1)/Smad signaling pathway.

Methods: The study explored the in vitro effects of near infrared (NIR) light on cell viability (survival) and proliferation as well as the presence of TGF-β1, phosphorylated TGF-β receptor type I (pTGF-βR1) and phosphorylated mothers against decapentaplegic-homolog (Smad)-2/3 (p-Smad2/3) in different fibroblast cell models.

Results: Results show a significant increase in cellular migration in wounded models, and increased viability and proliferation in irradiated cells compared to their respective controls. An increase in the presence of TGF-β1 in the culture media, a reduction in pTGF-βR1 and a slight presence of p-Smad2/3 was observed in the cells.

Conclusion: These findings show that PBM at 830 nm using a fluence of 5 J/cm^2 could induce cell viability, migration and proliferation to favor successful healing of diabetic wounds. This study contributes to the growing body of knowledge on the molecular and cellular effect of PBM and showcases the suitability of PBM at 830 nm in managing diabetic wounds.

Keywords: diabetic wound, photobiomodulation, wound healing, hyperglycemia, NIR light

Introduction

Globally, diabetes mellitus (DM), which was initially dubbed as a disease of the rich, is ravaging low- and middle-income populations. According to the 2021 International Diabetes Federation (IDF) report, 537 million adults are living with diabetes globally (75% of these adults live in low- and middle-income countries) and this figure is expected to increase to 643 million by 2030 and 753 million by 2045.[1] Africa has seen a significant increase in the incidence of DM, with an estimated 19.4 million adults living with diabetes (3.9% prevalence rate).[2] Unfortunately, the African region has the highest proportion of individuals living with diabetes who are unaware of their condition (approximately 54%; that is 1 in 2 persons).[1] There is a postulated increase of 129% in diabetic cases in Africa by the year 2045.[1] Data has suggested that this increase is connected to rapid demographic, sociocultural and economic transitions.[3]

With an increase in diabetes comes a rise in micro- and macrovascular complications, which could negatively impact the health of diabetic patients. This together with neuropathy leads to further complications and an increase in the incidence of lower limb amputations due to non-healing diabetic foot ulcers (DFUs).[4] Globally, it is estimated that 25% of the diabetic patients develop a DFU,[5] with a high recurrence rate of up to 70% within 5 years, and with statistics showing that 85% of the amputations in diabetics starts with ulcers.[6,7] Diabetic foot amputation is one of the most common and most feared complication of diabetes.[8] In certain parts of the world, like the USA, over one billion dollars is spent annually on managing chronic diabetic wounds.[9] Under diabetic conditions, alterations in any stage of wound healing could lead to slow or non-healing of even the most minor wounds, particularly on the body's lower extremities.[10] Wound healing in healthy individuals usually occurs through four clear-cut phases: hemostasis, inflammation, proliferation, and maturation (remodeling).[11] However, in DM, the wound healing process typically ceases at the inflammatory

Received: 21 May 2022
Accepted: 2 August 2022
Published: 21 September 2022

phase,[12] probably due to hyperglycemia which causes glucose to clog up the arteries and impede blood circulation, induce hypoxia, and inhibit collagen production.[13,14] A hyperglycemia-induced increase in reactive oxygen species (ROS) further promotes diabetic complications by increasing oxidative stress which could lead to tissue damage, weakened skin, and slow wound contraction.[15,16]

Growth factors, such as transforming growth factor beta (TGF-β) are involved in the process of wound closure through stimulation or inhibition of growth, proliferation and differentiation of fibroblast cells into myofibroblasts, thereby improving the formation of the extracellular matrix (ECM).[17] TGF-β together with its receptor and Smad constitute the TGF-β/Smad signaling pathway which can facilitate collagen synthesis, skin remodeling, and improve wound healing in fibroblast cells.[18] These activities are performed through isoforms of TGF-β which elicit their role via the Smad signaling pathway.[19] Cross-talk of the Smad signaling pathway with other signaling pathways (such as Wnt, Notch, Hippo, Hedgehog (Hh), mitogen-activated protein kinase (MAPK), phosphoinositide 3-kinase (PI3K)-Akt, nuclear factor kappa B (NF-κB), and JAK-STAT) play a role in the regulation of various biological processes, including wound healing.[19] The phosphorylation and recruitment of TGF-β receptor type I (TGF-βR1) occurs through the binding of TGF-β to its cell surface receptor TGF-β type II (TGF-βR2) to form a heterometric receptor complex.[20] The formed complex then phosphorylates Smad 2 and Smad 3 which in turn binds to Smad 4, initiating its nuclear translocation and expression of alpha smooth muscle actin (α-SMA) concomitantly activating genes responsible for cell proliferation, survival, and differentiation, which favors the healing of diabetic wounds.[21]

The impact of delayed wound healing, and ultimately loss of a limb in diabetic patients, creates a need for strategies to speed up the wound healing process. Most methods employed involve wound debridement (clean up and excision of infected and dead skin) to encourage migration and proliferation of healthy cells and to eliminate the spread of infection in the wound area.[22,23] A practical and alternate method in the treatment of diabetic wounds is the administration of low-energy light in the form of lasers or light-emitting diodes (LEDs) in a process known as photobiomodulation (PBM).[24] This process is painless and modulates cellular and biological pathways to speed up wound healing and is effective only when the correct fluence and wavelength/s are used in the correct combination.[25,26] Furthermore, PBM has been reported to alleviate oxidative stress by increasing antioxidant activity and reducing the intracellular production of ROS.[27] Specifically, research has been conducted on red (620–750 nm) and near-infrared (NIR) (780–950 nm) wavelengths to influence wound healing.[28] NIR light is found to be effective and is widely studied in the area of wound healing since this wavelength can penetrate deeper into tissues.[25] An increase in cell viability, migration, and proliferation has been reported to be induced by PBM at a wavelength of 660 nm (visible red light) and fluence of 5 J/cm^2 in vitro.[29,30] A study by Mokoena et al, 2019[31] showed that irradiation at a wavelength of 660 nm with a fluence of 5 J/cm^2 was successful in accelerating wound healing via the differentiation of fibroblasts into myofibroblasts, although this was done without activation of the TGF-β/Smad pathway. Considering the complexities that typify the wound healing process, there is a need to further understand how wavelength and fluence modulate molecular pathways during PBM. This will assist researchers and medical practitioners in choosing a suitable wavelength and dosage for effective diabetic wound healing. The rationale for using a NIR wavelength in this study is to add to the body of knowledge since most studies conducted in vitro were reported using red light and more studies on the biological effects of PBM using NIR light is required.[29–31] This study therefore aims to investigate the potential of PBM using a NIR wavelength at 830 nm and a fluence of 5 J/cm^2 in modulating TGF-β/Smad signaling pathway and improving wound healing process in normal, diabetic, and hypoxic in vitro wound models.

Materials and Methods

Cell Culture and Laser Irradiation

A human skin fibroblast cell line, WS1 (ATCC®, CRL-1502™), was used for this study and ethical clearance was obtained from the Faculty of Health Sciences, University of Johannesburg, Research Ethics Committee (REC-538-2020). Cells were grown in supplemented minimum essential media (MEM), as previously reported.[16] Five cell models were utilized in this study, namely normal (N) unstressed cells; normal wounded (NW); diabetic (D); diabetic wounded (DW); and hypoxic diabetic wounded (HDW). A diabetic model was induced by continuously growing cells in complete MEM with an additional 17 mM D-glucose (which brings the total glucose concentration to 22 mM).[26] Prior to irradiation, the hypoxic

Table 1 Laser Parameters

Variables	Current Study
Wavelength (nm)	830
Light source	Diode laser
Wave emission	Continuous wave
Spot size (cm^2)	9.1
Power output (mW)	105
Power density (mW/cm^2)	11.54
Irradiation time	7 min 10s
Energy density (J/cm^2)	5
Energy (J)	45.5

diabetic model (HDW) was attained by growing cells in media without fetal bovine serum (FBS) for 24 h and then followed by incubating the cells in an anaerobic jar for 4 h; an anaerobic indicator was used to validate the process.[32] For all experiments, except the proliferation assay, cells at a seeding density of 6×10^5 were irradiated in 3.4 cm diameter tissue culture plates followed by incubation at 37 °C in 5% CO_2. For the proliferation assay, 1×10^6 cells were seeded and kept under the same conditions. Thirty minutes pre-irradiation, a wound was stimulated via the central scratch using a 1 mL pipette in wounded models.[16,33,34] Creating a scratch on the cell monolayer serves as a valuable tool for understanding the effect of the experimental assays for promoting wound healing.[35] The scratch assay is cost effective and involves a simple experimental design thereby making it an invaluable method for understanding cell migration favoring the quantification of cell migration under controlled experimental conditions. A scratch assay is done by growing the cells to confluence and creating a "wound" (cell-free zone) on the cell monolayer to which the cells can migrate.[36]

The experimental groups were irradiated with a continuous wave diode laser provided by the Council for Scientific and Industrial Research (CSIR) – National Laser Centre (NLC) of South Africa (wavelength 830 nm; Fremont, California, RGBlase, TE-CIRL-70G-830 SMA), laser parameters are reported in Table 1. Cells (in 1 mL of culture medium) were irradiated in the dark with the laser beam targeted overhead the 3.4 cm diameter culture dish. A wavelength of 830 nm and a fluence of 5 J/cm^2 was used, as it has been reported to stimulate wound healing in WS1 cells in earlier studies.[26,37] An irradiation time of 7 min 10s was calculated based on the power output and power density of the laser (Table 1) to achieve the desired fluence of 5 J/cm^2. Non-irradiated cells (0 J/cm^2) functioned as controls. Cells were incubated for 24, 48 and 72 h post-irradiation.

Cellular Migration Rate

Cellular migration in the direction of the central scratch was observed. The rate of cell migration towards the central scratch was investigated in normal wounded (NW), diabetic wounded (DW) and hypoxic diabetic wounded (HDW) cells at 0, 24, 48 and 72 h through periodic microscopy via the Carl Zeiss Axio Observer Z1. The measurements were taken on the same spot in three different images, and the mean distance used for the calculations. Migration rate is expressed in percentage using the following equation:

$$(At_{oh} - At_{time}) / At_{oh} \times 100 \quad (1)$$

where At_{0h} represents measurements between boundaries of the scratch at 0 h and At_{time} is the measurement within the boundaries of the scratch at different times.[38]

CellTiter-Glo® Luminescent Cell Viability Assay

The CellTiter-Glo luminescent assay (Promega, G7571) is a consistent technique for measuring cell viability through the quantification of adenosine triphosphate (ATP) present in metabolically active cells. This technique measures luminescence obtained through the transformation of intracellular ATP to adenosine monophosphate (AMP) by the enzymatic action of luciferase, which signals the presence of metabolically active and viable cells.[28] Post-irradiation (24, 48 or 72 h), cells were detached and resuspended at 50,000 cells per 50 µL and the same volume of reagents were mixed in a 96-well plate for 2

min to generate cell lysis followed by 10 min incubation at room temperature. Luminescence was recorded on a Victor3™ multilabel plate reader (PerkinElmer) in relative light units (RLU).

ApoTox-Glo™ Triplex Assay

The ApoTox-Glo triplex assay (Promega, G6320) is more complex and is centered on the proteolytic action of biomarkers present in the cell. It was used to evaluate cell viability, cell cytotoxicity, and caspase 3/7 activation (a marker of apoptosis) 24, 48 or 72 h post-irradiation. Briefly, 100 µL of cell suspension (containing 20, 000 cells per 100 µL) was introduced into an opaque-walled 96-well plate and 20 µL of mixed glycyl phenylalanyl-amino fluorocoumarin (GF-AFC) and bis-alanylalanyl-phenylalnyl-rhodamine 100 (bis-AAFR110) substrate (viability/cytotoxicity reagent) was added. This mixture was combined for 30 s by orbital shaking (350 rpm) followed by incubation at 37 °C for 1 h, then fluorescent signals were measured using the PerkinElmer Victor3™ multilabel plate reader at 400EX/505EM (filters for viability) and 485EX/520EM (filters for cytotoxicity). Caspase 3/7 activity was subsequently quantified by adding 100 µL Caspase-Glo® 3/7 reagent to all wells, followed by incubation for 30 min at room temperature and measurement of luminescence in RLU. Background fluorescence was eliminated by subtracting the fluorescence of media without cells.

Cell Proliferation

The BD Pharmingen™ BrdU FITC Flow Kit (BD Biosciences, 559619/557891) was utilized to evaluate cell proliferation. The assay was performed according to the manufacturer's protocol and analyzed through flow cytometry using the BD Accuri C6. Following laser irradiation (24, 48, or 72 h), cells were stained with 30 µL of 1 mM BrdU for 1 h (BrdU incorporates into freshly synthesized DNA during the S-phase of the cell cycle), then detached from the culture plates using TrypLE™ Select (Gibco, 12563–029). Cells were suspended in BD Cytofix/Cytoperm™ buffer followed by 30 min incubation on ice. Cells were then washed with BD Perm/Wash™ buffer and centrifuged for 5 min at 300 g. Pellets were re-suspended in BD Cytofix/Cytoperm™ buffer followed by incubation on ice for 10 min. Cells were then washed and centrifuged as before and the pellet resuspended and incubated in DNase (300 µg/mL) in phosphate-buffered saline (PBS) for 1 h at 37 °C. Cells were washed as before and BD Perm/Wash™ buffer containing diluted fluorescent anti-BrdU antibodies was added, and incubated at room temperature for 20 min. A repeat washing process preceded the suspension of cells in 1 mL staining buffer mixed with 20 µL of 7-amino-actinomycin D (7-AAD). BrdU-labelled cells were counted via flow cytometry at a frequency of 400 events per second, with a sample limit set at 500 µL.

ELISA Assays

The release of TGF-β1 into the culture medium was analyzed using the Human TGF-β1 DuoSet® ELISA kit (R&D Systems; DY240), while the phosphorylation of Smad2/3 in the cells was detected using the InstantOne™ ELISA kit (Invitrogen, 85–86192). Both assays were performed using the kit protocol, and colometric reactions were measured spectrophotometrically at 450 nm using the PerkinElmer Victor3™ multilabel plate reader.

The presence of pTGF-βR1 in cultured cells was detected using a cell-based ELISA. Briefly, 100 µL of cell suspension (containing 20,000 cells per 100 µL) was introduced into 96-well microplates and incubated overnight to favor adherence of the cells. Then, the cells were fixed at room temperature for 15 min with 8% paraformaldehyde followed by washing with phosphate buffer and 0.1% tween-20 (PBS-T) and blocking with 5% bovine serum albumin, BSA and 0.05% sodium azide in PBS-T at room temperature for 2 h. Thereafter the cells were washed with PBS-T and a polyclonal primary antibody (1:200) for phosphorylated TGF-βR1 (Elabscience, ENO1191) was added. The mixture was incubated for 2 h at room temperature. This was followed by a washing step and then incubation with a secondary antibody 1:1000 (R&D Systems HAF008) for 2 h at room temperature. Then, the plates were washed and incubated for 20 min with 3,3′,5,5′-tetramethylbenzidine (TMB) and measured at 450 nm using a spectrophotometer (Victor3™ PerkinElmer).

Statistical Analysis

All experiments were performed in triplicate (n = 3), and results are expressed as the mean ± standard error of mean (SEM). Statistical significance was analyzed using SPSS version 27. Significant differences were determined by the

Student's *t*-test (control vs experiment) and one-way analysis of variance (ANOVA) (comparing between cell groups) and two-way ANOVA (comparing between irradiation and non-irradiation, irrespective of cell models). In all cases, p values of less than 0.05 were considered statistically significant.

Results

Cellular Migration Rate

The rate of cellular migration was investigated at 24, 48 and 72 h following laser irradiation and is shown in Table 2. The WS1 cells grown in a confluent monolayer appeared thin and spindle-like (Figure 1A).

Irrespective of the cell model, the rate of migration in irradiated cells was significant at both 24 and 48 h ($p = 0.0181$ and $p = 0.0001$) compared to non-irradiated cells (Table 2). At 24 h, the rate of migration in the NW cells was not significant ($p = 0.887$) compared to the DW cells, while compared to the HDW ($p = 0.05$), there was a slight significance increase in the rate of migration. At 48 h, the rate of migration in irradiated NW cells was significantly ($p = 0.016$ and $p = 0.0001$) lower in comparison to both irradiated DW and HDW cells.

Irradiated NW, DW and HDW cells displayed faster migration towards the central scratch compared to their non-irradiated control cells (Figure 1A-C). The distance written on the figures is the representative mean of the distance measured for each group. DW and HDW cells irradiated at 830 nm with 5 J/cm^2 depicted complete wound closure at 48 h, while NW cells only became fully confluent at 72 h (Figure 1A). Unirradiated control cells only showed complete wound closure at 72 h. In general, cellular migration was significantly improved in irradiated cells.

CellTiter-Glo Luminescent Cell Viability Assay

Cellular viability was determined using the CellTiter-Glo luminescent cell viability assay in all non-irradiated and irradiated cell models, and results can be seen in Figure 2. In general, there was a significant increase in ATP bioluminescence in irradiated cells irrespective of cell model when compared to non-irradiated cells at 24, 48 and 72 h ($p = 0.001$, $p = 0.01$ and $p = 0.001$, respectively). At 24 h, irradiated NW cells showed a significant ($p = 0.025$ and $p = 0.001$) increase in viability when compared with irradiated DW and HDW cells. There was also a significant increase in viability in irradiated N cells as compared to irradiated D and HDW cells ($p = 0.04$ and $p = 0.0001$), indicating the debilitating effect of hyperglycemia and hypoxia on cellular viability (as expected). At 48 h, irradiated NW cells showed a significant ($p = 0.001$) increase in viability as compared to irradiated HDW cells, while at 72 h, viability was significantly ($p = 0.0001$) higher in irradiated NW cells in comparison with DW and HDW cells.

ApoTox-Glo Triplex Assay

The ApoTox-Glo triplex assay was used to measure cellular viability, cytotoxicity and apoptosis in all non-irradiated and irradiated cell models, and results can be seen in Figures 3-5, respectively. Cell viability was significantly increased due to irradiation irrespective of cell model (Figure 3), at 24, 48 and 72 h ($p = 0.001$, $p = 0.002$ and $p = 0.0001$, respectively). At 24 and 48 h there was a significant ($p = 0.001$) increase in viability in N cells as compared to D cells. Furthermore,

Table 2 Cell Migration Rate (%) in Normal Wounded (NW), Diabetic Wounded (DW) and Hypoxic Diabetic Wounded (HDW) Cells After Irradiation at 830 Nm with 5 J/cm^2 at 24, 48, and 72 h Compared with Their Corresponding Non-irradiated (0 J/cm^2) Wounded Models

Incubation Time After Irradiation						
	24 h		48 h		72 h	
Models	0 J/cm^2	5 J/cm^2	0 J/cm^2	5 J/cm^2	0 J/cm^2	5 J/cm^2
NW	26.8 ± 1	43.2 ± 3*	80.7 ± 2	84.1 ± 1	100	100
DW	19.0 ± 2	43.1 ± 3*	78.4 ± 1	100***	100	100
HDW	40.1 ± 4	44.2 ± 1	73.5 ± 2	100**	100	100

Note: *p < 0.05, **p < 0.01 and ***p < 0.001 (±SEM) represents statistical significance when compared to non-irradiated cells.

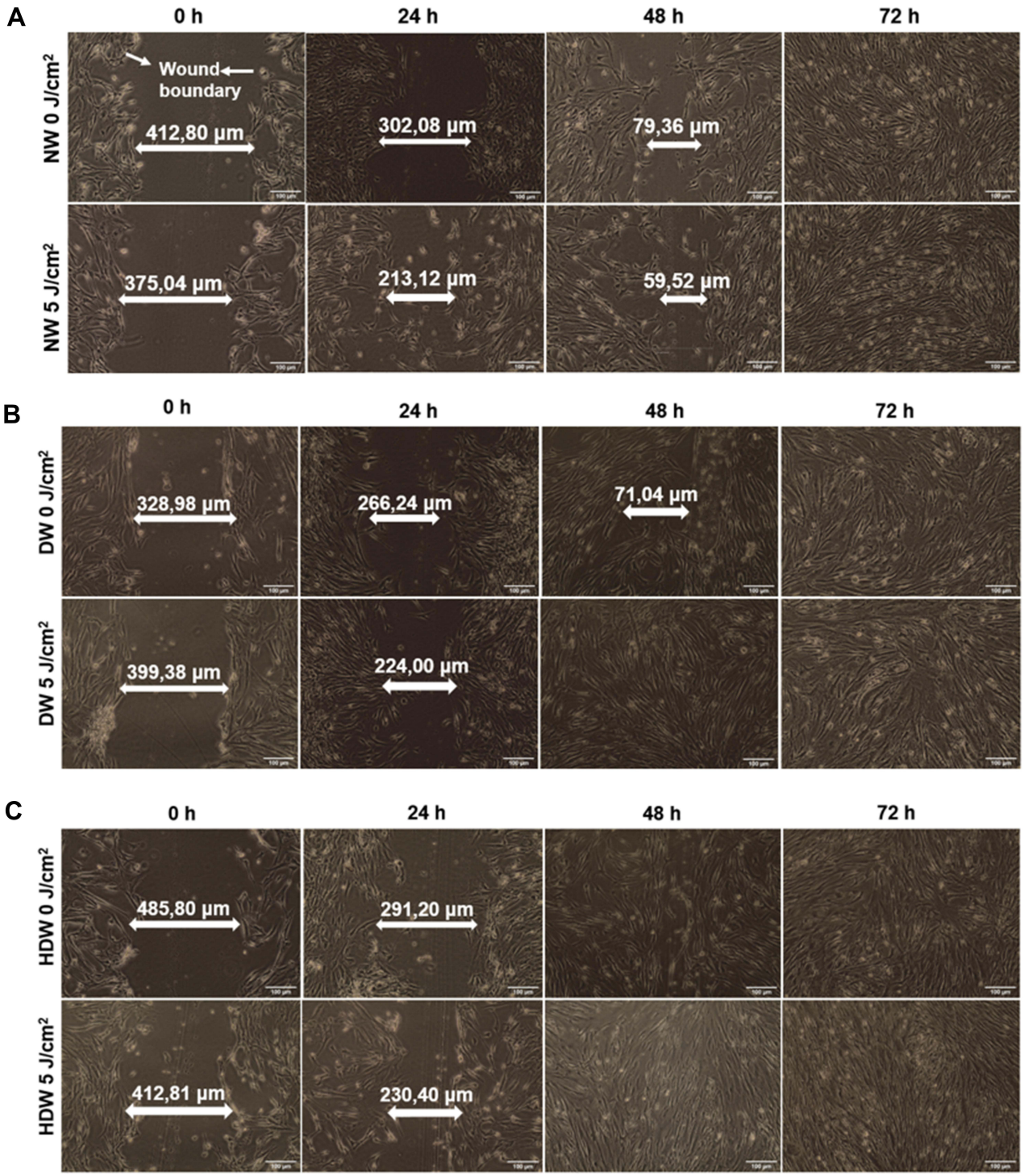

Figure 1 (**A**) Normal wounded (NW), (**B**) Diabetic wounded (DW) and (**C**) Hypoxic diabetic wounded (HDW) WS1 fibroblast cells at 0, 24, 48, and 72 h post-irradiation at 830 nm with 5 J/cm^2 (magnification 200x, scale bar = 200 µm), non-irradiated (0 J/cm^2) cells served as controls.

viability was significantly ($p = 0.0001$ and $p = 0.002$) higher in irradiated NW cells compared to the irradiated HDW cells at 24 and 48 h. At 72 h irradiated NW cells showed a significant increase in viability in comparison with irradiated DW and HDW cells ($p = 0.0001$).

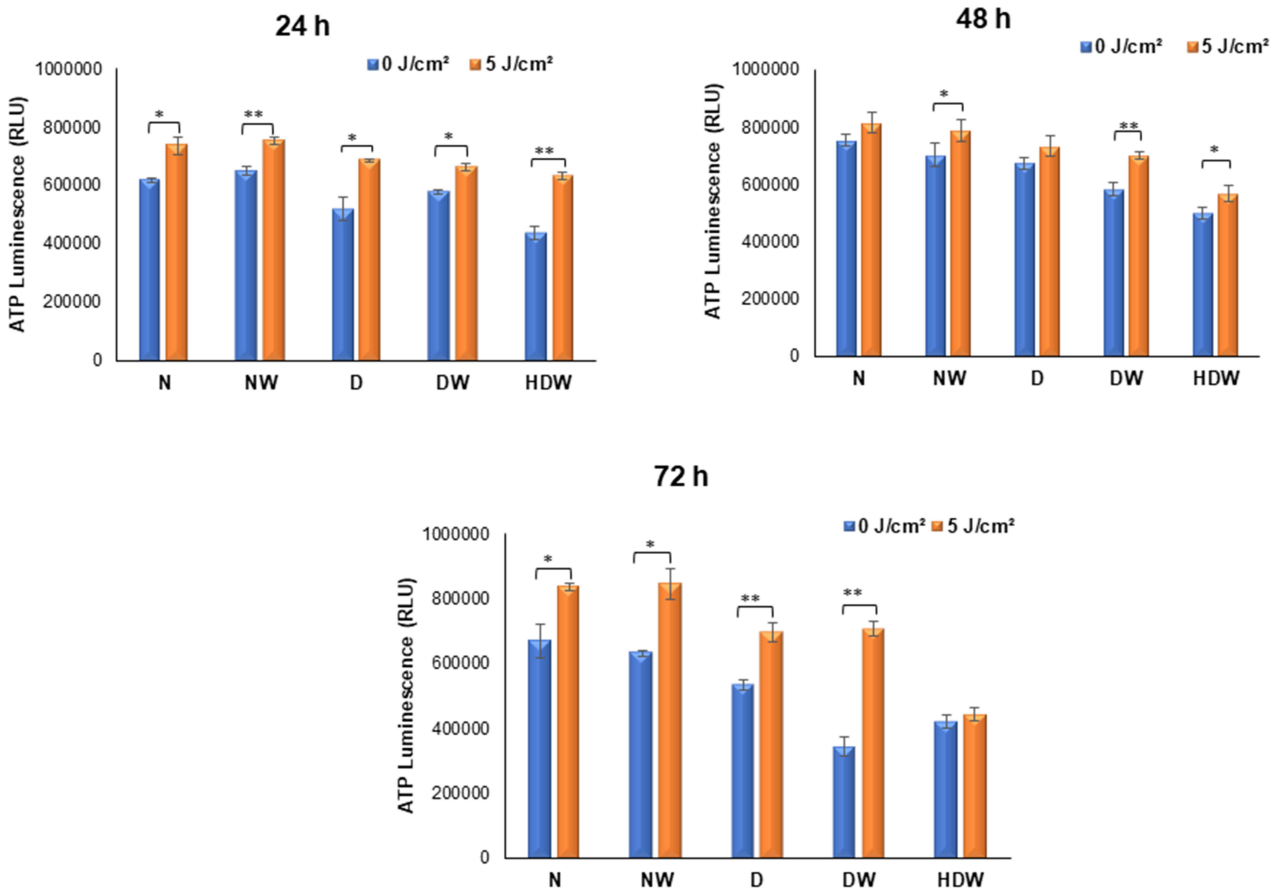

Figure 2 Cellular viability as evaluated by the CellTiter-Glo luminescent cell viability assay (ATP luminescence measured in relative light units, RLU).
Notes: Luminescence was recorded in irradiated (5 J/cm^2) and non-irradiated (0 J/cm^2) normal (N), normal wounded (NW), diabetic (D), diabetic wounded (DW) and hypoxic diabetic wounded (HDW) cells and analyzed 24, 48 and 72 h post-irradiation (830 nm). *$p < 0.05$ and **$p < 0.01$ (±SEM) represent statistical significance when compared to non-irradiated cells.

Just as irradiation increased cell viability, it was also able to reduce cell cytotoxicity irrespective of the models at 24, 48 and 72 h ($p = 0.0001$, $p = 0.001$ and $p = 0.0001$, respectively) (Figure 4). At 24 h, irradiated NW cells showed a significant ($p = 0.001$ and $p = 0.007$) decrease in cytotoxicity compared to irradiated DW and HDW cells, while at 48 h no significant difference ($p = 0.750$ and $p = 0.161$) was observed. However, at 72 h, cytotoxicity in irradiated NW cells was significantly ($p = 0.001$ and $p = 0.0001$) increased compared to in irradiated DW and HDW cells.

Irrespective of cell model, irradiation at 830 nm resulted in a reduction in caspase 3.7 activation at 24, 48 and 72 h ($p = 0.0001$, $p = 0.027$ and $p = 0.02$, respectively) (Figure 5). At 24 h, irradiated N cells showed a significant increase in the activation of Caspase 3/7 compared to the irradiated D cells ($p = 0.01$), while there was no significant ($p = 1.00$ and $p = 0.569$) difference in irradiated NW cells compared to DW and HDW cells. At 48 h, irradiated NW cells showed no significant ($p = 1.00$ and $p = 0.756$) difference in caspase 3/7 activation as compared to irradiated DW and HDW cells. While at 72 h irradiated NW cells showed a significant ($p = 0.046$ and $p = 0.017$) decrease in caspase 3/7 activation as compared to irradiated DW and HDW cells.

Cell Proliferation

BrdU incorporation into non-irradiated and irradiated cells was used to determine cell proliferation, and changes were observed at 24, 48 and 72 h (Table 3) post-irradiation using a flow cytometer. Irrespective of cell model, irradiation at 830 nm with 5 J/cm^2 produced no significant difference in the percentage of cells in the G0/G1 (resting/gap) phase at 24, 48 and 72 h ($p = 0.581$, $p = 0.829$, and $p = 0.094$, respectively), which signals the continuous activity of these cells. At 24 h, the

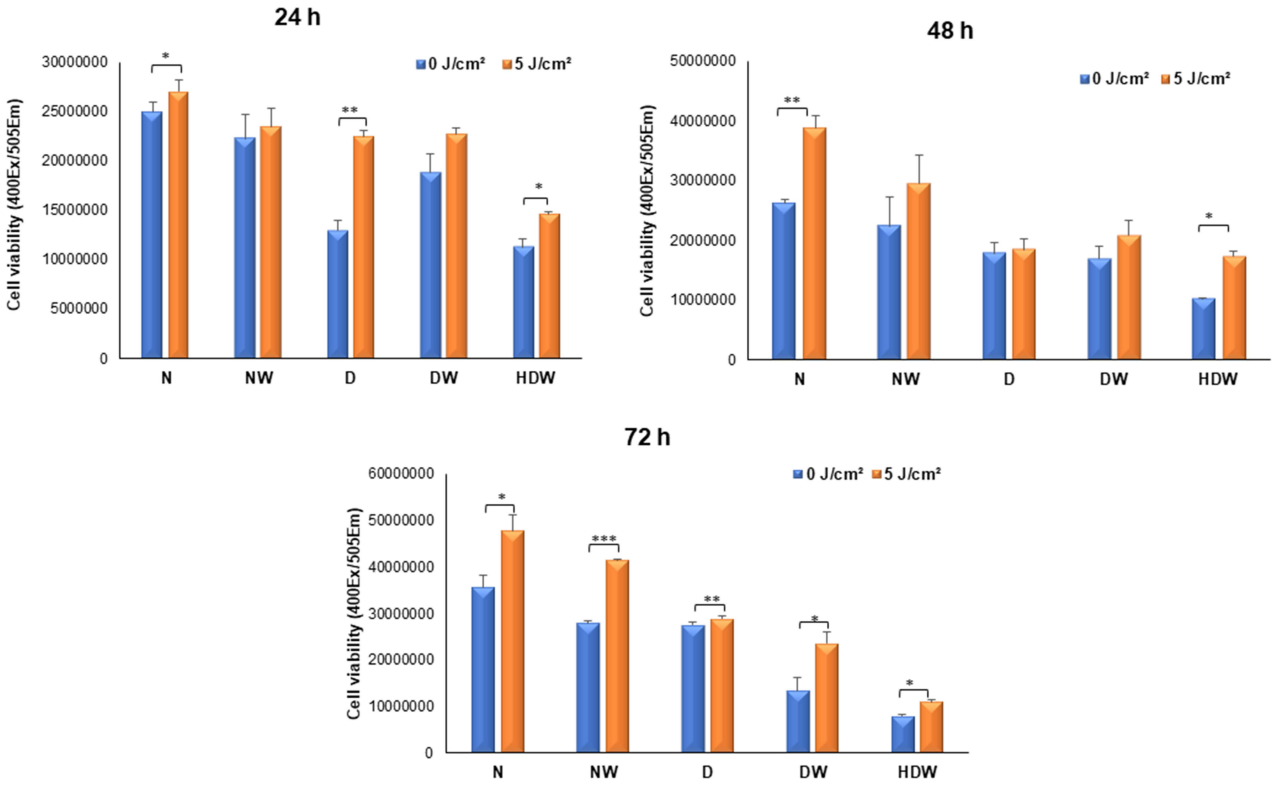

Figure 3 Cellular viability as assessed by the ApoTox-Glo triplex assay in WS1 cells.
Notes: Cell viability was measured in irradiated (5 J/cm^2) and non-irradiated (0 J/cm^2) normal (N), normal wounded (NW), diabetic (D), diabetic wounded (DW) and hypoxic diabetic wounded (HDW) cells and analyzed 24, 48 and 72 h post-irradiation (830 nm). *p < 0.05, **p < 0.01 and ***p < 0.001 (±SEM) represent statistical significance when compared to non-irradiated cells.

percentage of cells in the G0/G1 phase in the irradiated NW group was significantly (p = 0.003) higher compared to irradiated HDW cells, while there was no significant (p = 0.258) difference when compared to DW cells.

In the S-phase, irradiation at 830 nm with 5 J/cm^2 resulted in a significant increase in cell proliferation compared to non-irradiation at 24, 48 and 72 h (p = 0.001, p = 0.0001, and p = 0.0001, respectively), irrespective of cell model. At 24 h, irradiated NW cells showed a significant (p = 0.002) decrease in proliferation compared to irradiated DW cells; no significant (p = 0.952) difference was seen when compared to irradiated HDW cells. However, at 48 and 72 h, proliferation was significantly (p = 0.001) higher in irradiated NW cells compared to irradiated DW and HDW cells.

In the G2/M (checkpoint for mitotic activity) phase, irradiation produced no significant (p = 0.459, and p = 0.893) difference at 24 and 48 h irrespective of cell model, while at 72 h there was a significant increase in irradiated cells (p = 0.0001) compared to non-irradiated cells. At 24 h, the percentage of cells in the G2/M phase in irradiated NW cells was significantly (p = 0.0001) higher compared to irradiated HDW cells. At 48 h, no significant (p = 0.999 and p = 1.00) difference was seen when irradiated NW cells was compared to irradiated DW and HDW cells, while at 72 h the difference in irradiated NW cells was significantly (p = 0.001 and p = 0.0001) higher compared to irradiated DW and HDW cells.

ELISA Results

ELISA was used to determine TGF-β1 levels in the culture media, and results can be seen in Figure 6. Irrespective of cell groups, irradiation at 5 J/cm^2 caused a significant reduction in TGF-β1 levels (p = 0.001) at 24 h, while at 48 h and 72 h, TGF-β1 levels increased (p = 0.0001) significantly. At 24 h, irradiated NW cells showed no significant difference (p = 0.059 and p = 0.139) in TGF-β1 levels compared to irradiated DW and HDW cells. At 48 h there was no significant (p = 0.272 and p = 0.066) difference in TGF-β1 levels in irradiated NW cells compared to irradiated DW and HDW

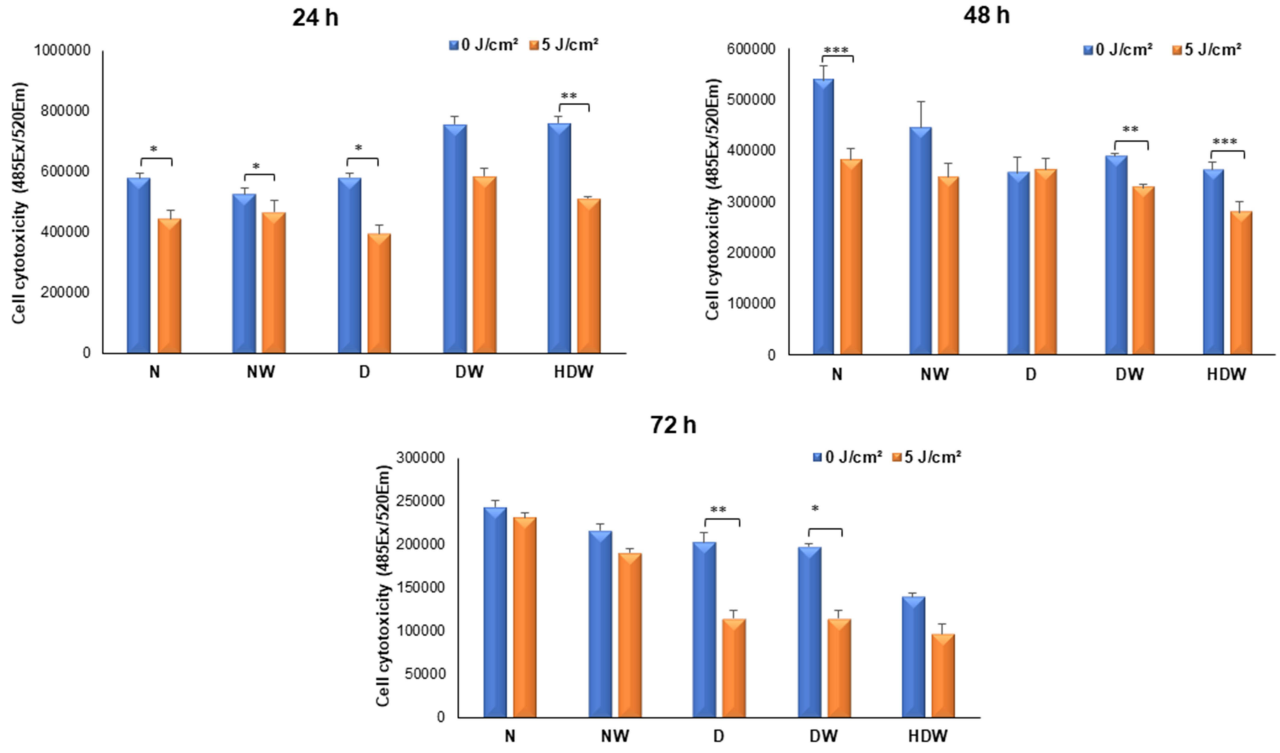

Figure 4 Cell cytotoxicity as assessed by the ApoTox-Glo triplex assay in WS1 cells.
Notes: Cytotoxicity was measured in irradiated (5 J/cm^2) and non-irradiated (0 J/cm^2) normal (N), normal wounded (NW), diabetic (D), diabetic wounded (DW) and hypoxic diabetic wounded (HDW) cells and analyzed 24, 48 and 72 h post-irradiation (830 nm). *p < 0.05, **p < 0.01 and ***p < 0.001 (±SEM) represent statistical significance when compared to non-irradiated cells.

cells. At 72 h, irradiated NW cells showed a significantly (p = 0.003) higher level of TGF-β1 compared to irradiated HDW cells.

The presence of phosphorylated (and hence activated) pTGF-βR1 was also measured via ELISA (Figure 7). Irrespective of cell groups, irradiation caused a significant reduction in pTGF-βR1 levels at 24 h, 48 h and 72 h (p = 0.0001, p = 0.004, and p = 0.004, respectively). At 24h, there was no significant (p = 0.547 and p = 0.936) difference in pTGF-βR1 levels in NW cells compared to DW and HDW cells, while at 48 h there was a significantly (p = 0.001) lower level of pTGF-βR1 in irradiated NW cells compared to irradiated DW cells. At 72 h, there was no significant (p = 187 and p = 0.161) difference in pTGF-βR1 levels in irradiated NW compared to irradiated DW and HDW cells.

Levels of phosphorylated (activated) p-Smad2/3 was measured via ELISA (Figure 8). Irrespective of cell groups, irradiation caused a significant (p = 0.0001) increase in p-Smad2/3 levels at 24 h only, while at 48 and 72 h there was no significant (p = 0.179 and p = 0.258, respectively) difference. In addition, at 24 h, irradiated NW cells showed a significantly (p = 0.0001) higher level of p-Smad2/3 compared to irradiated DW and HDW cells. At 48 h, irradiated NW cells showed significantly (p = 0.003 and p = 0.00002) higher p-Smad2/3 levels compared to irradiated DW and HDW cells. At 72 h, irradiated NW cells showed significantly (p = 0.002) lower p-Smad2/3 levels compared to irradiated DW cells.

Discussion

Many in vitro studies have highlighted the efficacy of PBM in altering processes for effective wound healing in diabetic cells.[28,30] These successes are likely due to PBM stimulating enhanced collagen synthesis and release of growth factors that facilitate successful wound repair processes.[28] Most findings on the effectiveness of PBM in diabetic wound healing utilize light in the red and NIR region of the electromagnetic spectrum. This is because tissue chromophores such as hemoglobin and melanin take up wavelengths shorter than 600 nm, thereby making the red and NIR region an optical therapeutic window where the efficiency of light penetration in the tissue is maximum.[39,40] The success of PBM is based

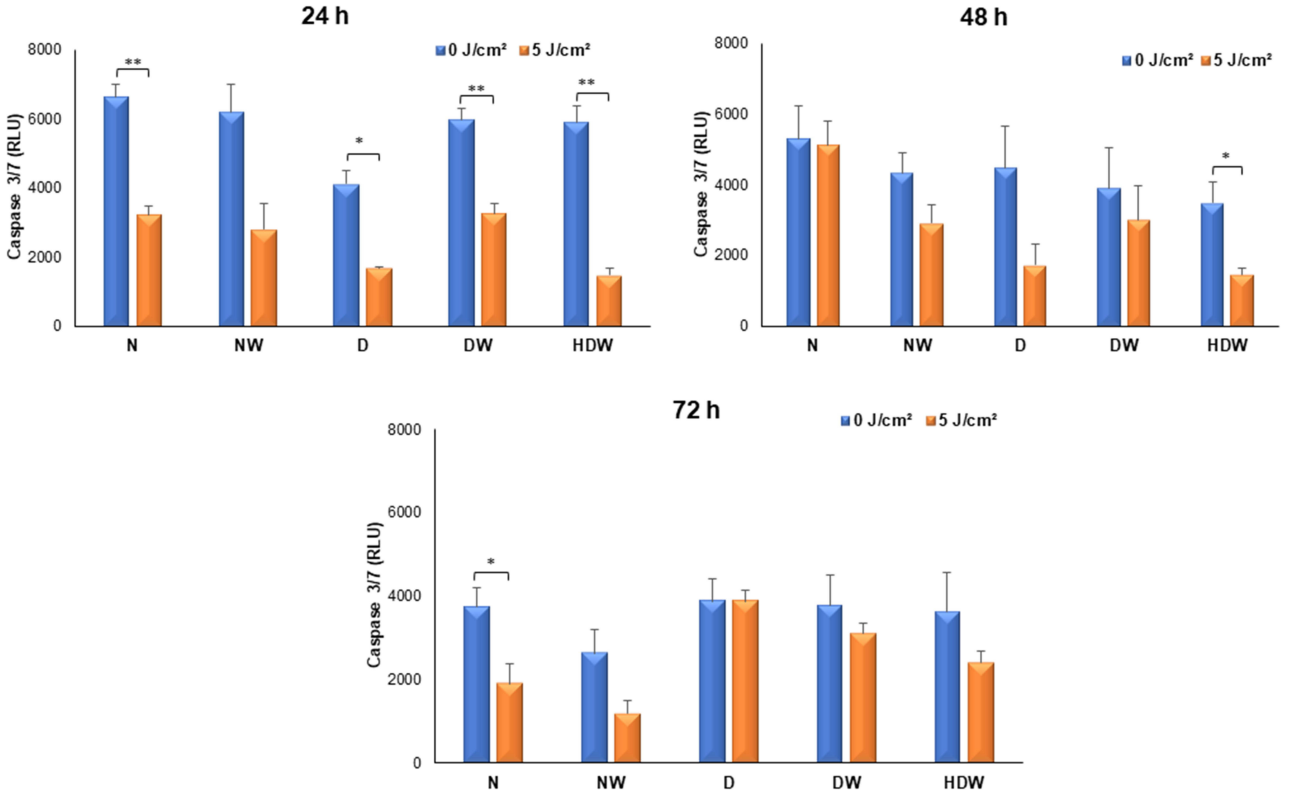

Figure 5 Caspase 3/7 activation as assessed by the ApoTox-Glo triplex assay in WS1 cells (expressed in RLU).
Notes: Caspase 3/7 activation was measured in irradiated (5 J/cm^2) and non-irradiated (0 J/cm^2) normal (N), normal wounded (NW), diabetic (D), diabetic wounded (DW) and hypoxic diabetic wounded (HDW) cells and analyzed 24, 48 and 72 h post-irradiation (830 nm). *p < 0.05 and **p < 0.01 (±SEM) represent statistical significance when compared to non-irradiated cells.

on using the correct wavelength, dose and fluence, although the exact dimensions of these parameters have not been ascertained. Studies using PBM at a visible red wavelength (660 nm) has shown an improvement in cell migration, viability, and proliferation in human diabetic fibroblast cells.[28,29] Cell viability and proliferation has been reported to be increased through PBM by increased production of nucleic acids for protein synthesis with an absence of cell damage or cytotoxicity.[33]

For this study, a NIR wavelength (830 nm) was used to investigate the release of TGF-β1 and subsequent activation of its receptor TGFβR1 and downstream p-Smad 2/3 and its effect on migration, viability and proliferation in relation to wound healing, since there is sparse information on the influence of this wavelength in promoting cell viability and proliferation. Also, irradiation at a NIR wavelength has been reported to improve diabetic wound healing in an in vivo animal study due to its depth of penetration into skin.[41] A fluence of 5 J/cm^2 was used for this study since it has been reported to be effective in improving diabetic wounds in WS1 fibroblast cells in vitro in earlier studies.[35,36,42]

Studies have shown that the migration and proliferation of dermal fibroblasts are essential to the formation of new tissue and remodeling in cutaneous wound healing.[43,44] The migration of fibroblasts and repopulation of cells at the wound site is an important step in wound healing,[45] and this is better understood using the central scratch assay. This assay allows for recolonization and monitoring of the scratched region to quantify cell migration.[46,47] This experimental technique of the scratch assay aids in the understanding of the molecular mechanisms that influence cell migration and identifying pharmaceutical compounds (or in this case light) that can induce cell migration.[48] One of the limitations of the scratch model include the absence of other cells that may be present at the site of a wound and the lack of cellular interactions with fibroblasts. Nevertheless, valuable information is obtained to better understand cellular mechanisms in an in vivo environment. Using microscopy, we investigated the rate of migration of cells into the central scratch in normal wounded, diabetic wounded, and hypoxic diabetic wounded cells 24, 48, and 72 h post-irradiation. The observed

Table 3 Cell Proliferation Was Determined by Flow Cytometry (% Cells in S, G0/G1 and G2/M Phase) in Non-Irradiated (0 J/cm^2) and Irradiated (5 J/cm^2) Normal (N), Normal Wounded (NW), Diabetic (D), Diabetic Wounded (DW) and Hypoxic Diabetic Wounded (HDW) Cells 24, 48 and 72 h Post-Irradiation at 830 Nm

	G0/G1 Phase		S Phase		G2/M Phase	
24 h	**0 J/cm^2**	**5 J/cm^2**	**0 J/cm^2**	**5 J/cm^2**	**0 J/cm^2**	**5 J/cm^2**
N	70.3 ± 2	76.7 ± 5.2	7.9 ± 0.3	13.2 ± 1.9	5.7 ± 1.5	7.8 ± 1.5
NW	73.5 ± 5.6	74.4 ± 1.9	8.1 ± 0.3	9.7 ± 0.7*	11.4 ± 1.5	11.2 ± 2.2
D	72.4 ± 3.2	71.4 ± 3.2	10.7 ± 0.4	13.3 ± 0.5***	9.1 ± 0.2	8.0 ± 1.0
DW	68.6 ± 2.1	65.5 ± 2.1	13.1 ± 0.7	13.9 ± 0.9	9.8 ± 0.3	12.8 ± 0.4*
HDW	58.9 ± 1.7	61.5 ± 0.3	8.4 ± 0.6	10.8 ± 0.4	3.7 ± 1.1	3.4 ± 0.6
48 h						
N	54.6 ± 4.7	46.5 ± 3.8*	16.0 ± 0.4	18.1 ± 1	4.8 ± 1.0	5.7 ± 1.1
NW	54.9 ± 3.6	54.3 ± 3.7	13.5 ± 0.5	16.7 ± 0.6**	4.5 ± 0.3	6.7 ± 1.2
D	50.8 ± 3.6	54.6 ± 4.5	10 ± 0.3	12.1 ± 0.6**	6.6 ± 1.2	4.9 ± 1.0**
DW	47.9 ± 4.4	50.4 ± 1.6	5.2 ± 0.4	7.6 ± 0.7**	6.9 ± 0.6	3.6 ± 1.0
HDW	50.8 ± 0.7	50.2 ± 1.7	4.2 ± 0.5	7.1 ± 0.9	4.6 ± 0.6	6.2 ± 0.5**
72 h						
N	54.3 ± 2.3	61.6 ± 2.0**	20.4 ± 0.7	26.1 ± 1.7*	2.5 ± 0.5	9.3 ± 0.4**
NW	53.1 ± 1.5	53.7 ± 1.5	17.1 ± 0.3	18.1 ± 0.2	5.2 ± 0.5	6.7 ± 1.0
D	49.6 ± 3.7	53.2 ± 1.8	11.9 ± 1.0	15.5 ± 0.4	4.3 ± 0.5	7.5 ± 0.4*
DW	54.1± 3.1	52.0 ± 2.0	8.1 ± 0.2	9.3 ± 0.4	4 ± 0.6	2 ± 0.2
HDW	48.3 ± 0.8	53.7 ± 1.0	6.0 ± 0.1	7.8 ± 0.3**	1.7 ± 0.2	2.6 ± 0.5

Note: *p < 0.05, **p < 0.01 and ***p < 0.001 (±SEM) represents statistical significance when compared to non-irradiated cells.

general physical appearance of the fibroblast cells in all the models seems consistent with the results reported in a similar study.[29] The cells appeared spindle-shaped with bi- or multipolar protrusions, and both the control and irradiated cells looked the same. Their migration was in the same direction with total closure of the "wound" seen at 72 h in the wounded cell models. A faster rate of migration was seen in the diabetic wounded and hypoxic diabetic wounded cells, with complete wound closure at 48 h. These results show that irradiation at 830 nm with 5 J/cm^2 significantly increases the migration rate of fibroblast cells and suggests that the stressed models reacted better to PBM. Irradiation at 5 J/cm^2 accelerated the rate of wound closure in our study, which is similar to results from studies that used the same wavelength (830 nm).[26,49] Fibroblast cells usually react to the disorganization of cell-to-cell communication by producing more growth factors at the wound site to facilitate healing through activation of both migration and proliferation.[45,50]

Our results from the cell viability assay using ATP luminescence showed a substantial increase in cell viability in all treated cell models over time. As expected, cell viability was reduced in the diabetic wounded and hypoxic diabetic wounded cells as compared to the normal and normal wounded cells. Hyperglycemia and hypoxia are stressors that induce cellular damage and senescence, hence the decrease in viability recorded in the stressed models. The ApoTox-Glo triplex assay further investigated the effect of laser irradiation at 830 nm on cytotoxicity and caspase 3/7 activation, which are markers of cell damage and progression to apoptosis, respectively. Our results showed that irradiation could reduce cytotoxicity and alter the activation of caspase 3/7, indicating that irradiation at 830 nm with 5 J/cm^2 had a protective effect on cell integrity. Increased cytotoxicity and activation of caspase 3/7 are triggers of apoptosis which signals cell death, irradiation mitigated the incidence of cell death while favoring cell viability. Interestingly, our results show a higher cytotoxicity and caspase 3/7 activity in non-irradiated cells compared to irradiated cells, this shows (in combination with the viability results) how PBM in general, significantly decreases cellular apoptosis with a concomitant

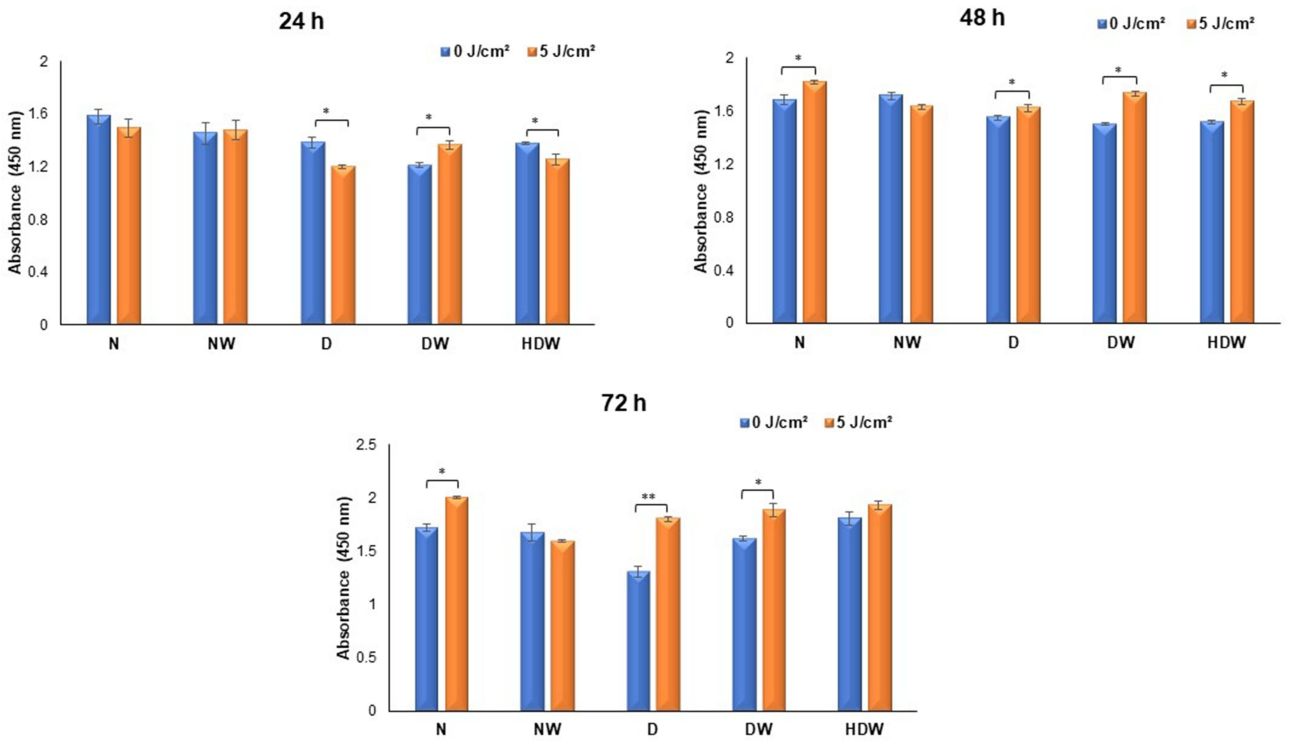

Figure 6 Presence of TGF-β1 in culture media measured using ELISA in irradiated (5 J/cm^2) and non-irradiated (0 J/cm^2) normal (N), normal wounded (NW), diabetic (D), diabetic wounded (DW) and hypoxic diabetic wounded (HDW) cells and analyzed 24, 48 and 72 h post-irradiation (830 nm).
Note: *p < 0.05 and **p < 0.01 (±SEM) represent statistical significance when compared to non-irradiated cells.

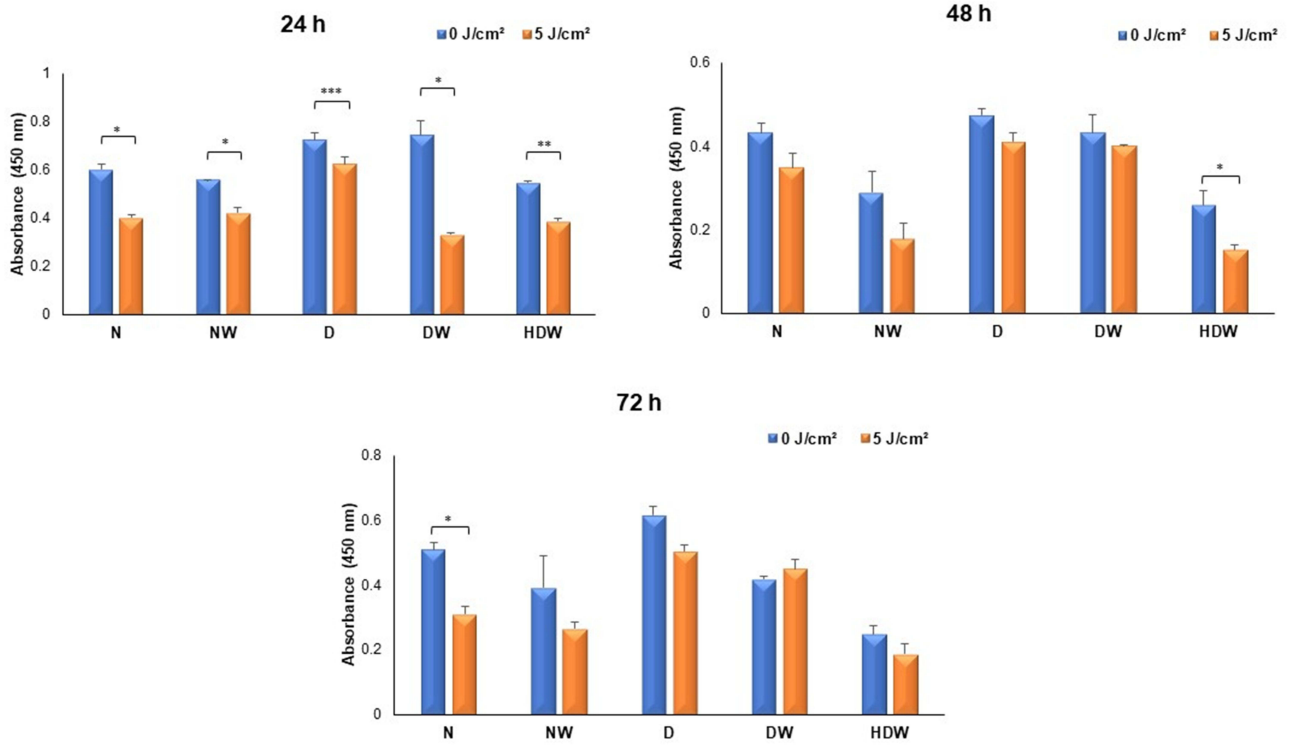

Figure 7 Presence of pTGF-βR1 measured using ELISA in irradiated (5 J/cm^2) and non-irradiated (0 J/cm^2) normal (N), normal wounded (NW), diabetic (D), diabetic wounded (DW) and hypoxic diabetic wounded (HDW) cells and analyzed 24, 48 and 72 h post-irradiation (830 nm).
Notes: *p < 0.05, **p < 0.01 and ***p < 0.001 (±SEM) represent statistical significance when compared to non-irradiated cells.

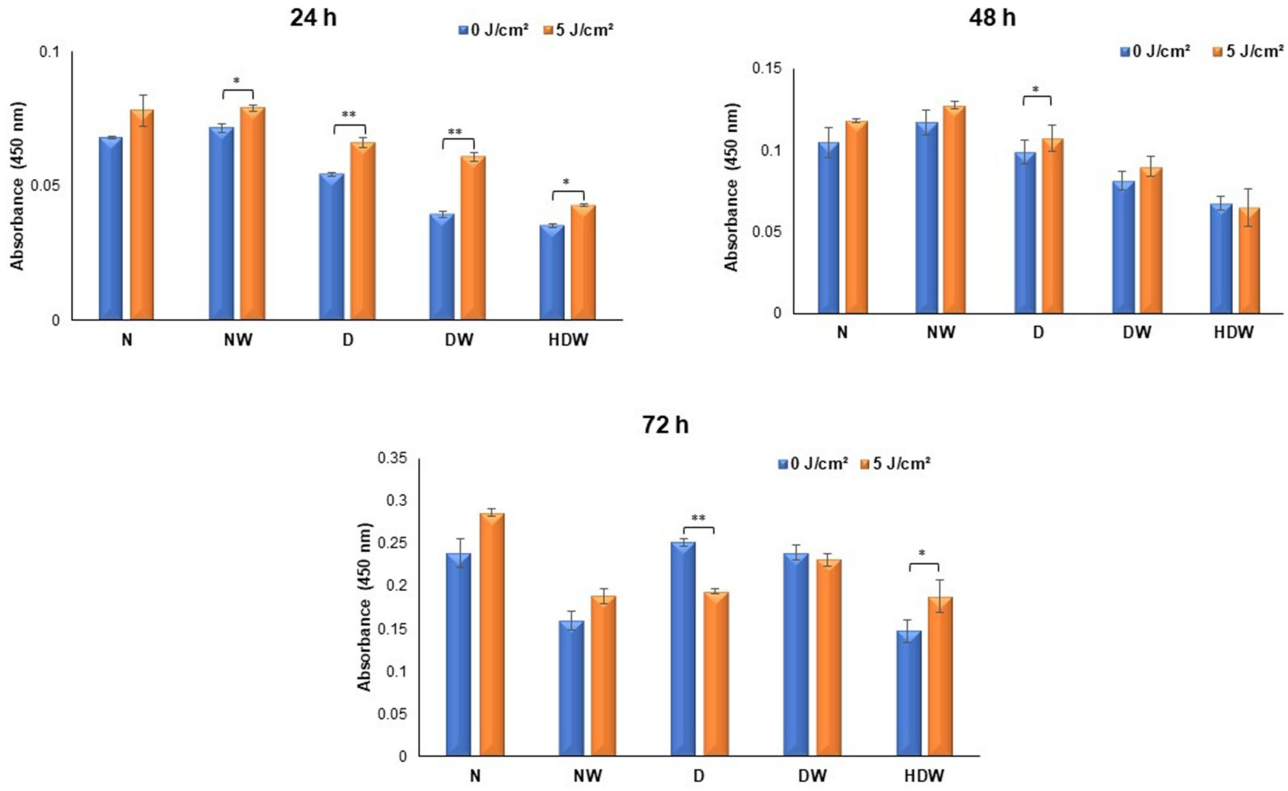

Figure 8 Presence of p-Smad2/3 measured using ELISA in irradiated (5 J/cm^2) and non-irradiated (0 J/cm^2) normal (N), normal wounded (NW), diabetic (D), diabetic wounded (DW) and hypoxic diabetic wounded (HDW) cells and analyzed 24, 48 and 72 h post-irradiation (830 nm).
Note: *p < 0.05 and **p < 0.01 (±SEM) represent statistical significance when compared to non-irradiated cells.

increase in cell viability and survival. Other studies have also reported that PBM using a NIR wavelength favors cell viability without generating any cytotoxic effects.[51,52]

The proliferation of fibroblast cells is an important factor in achieving successful wound healing. Increased cell migration and proliferation favor epithelial movement to cover the wound site.[53] Several changes occur in the expression pattern of key regulators of the cell cycle. Cell proliferation studies based on the cell cycle is successful when there is a surge in the S and G2M phase, which signals an advancement from the G1/S phase to a mitotic phase.[54,55] Our results showed that irradiation stimulated cells to enter and initiate the S and G2/M phase from the G0/G1 phase, which is an indication of the distribution of cells in different phases to favor the proliferation of the fibroblast cells, and it confirms findings from other studies using a different wavelength (660 nm).[16] These findings also support the results seen in the cell migration rate, wound closure, and viability assays. Studies have shown that the process of wound repair involves the interrelated activity of cell migration, viability, and proliferation.[56] The diabetic (D and DW) and HDW cells also showed an alteration in the G0/G1 phase, showing that their stressed state did not prevent them from partaking in the process of cell proliferation, which could indicate that irradiation improved their homeostasis that could aid in wound repair. Maintaining a balance between cell proliferation and cell death is crucial for tissue development and favors wound repair.

A better understanding of the cellular pathways involved in wound healing is key for the development of effective therapies for diabetic patients with chronic wounds. TGF-β acts as a growth factor that is effective in stimulating wound repair processes.[57] The major intracellular mediators of TGFβ family members are the Smad proteins which makes the TGFβ/Smad signaling pathway important for wound healing.[58] In this study, the observed increase in TGF-β1 levels at 48 and 72 h in irradiated cells suggests that TGF-β was released into the culture media. In vivo studies have reported that TGF-β-mediated chemotaxis can improve fibroblast proliferation and extracellular matrix (ECM) remodeling, and increase the accumulation of fibronectin and collagen at the wound site to favor successful wound healing.[59–61] Interestingly, some exogenous TGF-β-targeted in vitro experiments using monolayer cell cultures have reported that

the differentiation of fibroblasts into myofibroblasts can be induced by the presence of TGF-β and associated expression of alpha smooth muscle actin (α-SMA).[62,63] TGF-β has been reported to play a role in cell proliferation, differentiation, and proliferation in fibroblastic cells during angiogenesis.[64–66] Receptor-specific Smads (Smad 2 and Smad 3) are important proteins for TGF-β mediated signaling. The binding of TGF-β to its type I/type II receptor induces the type I receptor to phosphorylate the receptor-specific Smads which then forms an oligomeric complex with the common Smad (Smad 4) and subsequently aids in its translocation to the nucleus to regulate gene expression.[67] In our study, the decrease in the levels of pTGF-βR1 might suggest that the ELISA assay was not sufficient in detecting the presence of the activated receptor, Western blots and flow cytometry techniques could be used to better quantify the levels of the receptor in the cells. We could also suggest the possibility of TGF-β induced wound repair by binding to receptors other than TGF-βR1 to activate other non-Smad signaling pathways such as MAP kinase (MAPK), Rho-like guanosine triphosphatase (GTPase), and phosphatidylinositol-3-kinase (PI3K)/AKT.[68] The slight increase in p-Smad2/3 levels in the cells at 24 h is also not enough reason to justify that the TGF-β/Smad signaling pathway was activated and is responsible for viability and proliferation the cells. Other pathways initially mentioned might be responsible for the successful activation of the wound healing process. More research is needed to validate the initiation of the pathway.

This study has limitations in that it is done on a 2D cell culture model using a single-cell line, and the results represented here could be different in vivo.

Conclusion

The findings of this study confirm that PBM at a NIR wavelength of 830 nm and a fluence of 5 J/cm^2 improves the rate of cellular migration, viability, and proliferation most especially in diabetic, and excessively stressed hypoxic diabetic wounded cells (which had an absence of oxygen and presence of glucose), and decreases cellular apoptosis in stressed cells, contributing to the increase in cell viability. These observations could have occurred via the activation of another pathway other than the TGF-β/Smad signaling pathway, and further studies on other cellular signaling pathways using NIR light are warranted to better understand the mechanisms involved in PBM. These results show that PBM could serve an indispensable role in healing wounds of diabetic patients in dire conditions.

Funding

This work was supported by the South African Research Chairs Initiative of the department of Science and Technology and National Research Foundation of South Africa (Grant No. 98337), as well as grants received from the University of Johannesburg (URC), the National Research Foundation (NRF) and the Council for Scientific and Industrial Research (CSIR)-National Laser Centre (NLC) Laser Rental Pool Program.

Disclosure

The authors report no conflicts of interest in this work.

References

1. IDF. *International Diabetes Federation Atlas.*10th ed. Brussels, Belgium: IDF; 2021.
2. Saeedi P, Salpea P, Karuranga S, et al. Mortality attributable to diabetes in 20–79 years old adults, 2019 estimates: results from the International Diabetes Federation Diabetes Atlas. *Diabetes Res Clin Pract*. 2020;162:108086. doi:10.1016/j.diabres.2020.108086
3. Abbas ZG, Boulton AJM. Diabetic foot ulcer disease in African continent:' From clinical care to implementation'–Review of diabetic foot in last 60 years–1960 to 2020. *Diabetes Res Clin Pract*. 2022;183:109155. doi:10.1016/j.diabres.2021.109155
4. Riedel U, Schüßler E, Härtel D, et al. Wound treatment in diabetes patients and diabetic foot ulcers. *Hautarzt*. 2020;71:835–842. doi:10.1007/s00105-020-04699-9
5. Armstrong DG, Boulton AJM, Bus SA. Diabetic foot ulcers and their recurrence. *N Engl J Med*. 2017;376:2367–2375. doi:10.1056/NEJMra1615439
6. Peters EJG, Lipsky BA, Aragón-Sánchez J, et al. Interventions in the management of infection in the foot in diabetes: a systematic review. *Diabetes Metab Res Rev*. 2020;36:e3282. doi:10.1002/dmrr.3282
7. Abbas ZG. The Diabetic Foot Worldwide: sub-Saharan Africa. *Foot Diabetes*. 2020;25;51–60.
8. Sarfo-Kantanka O, Sarfo FS, Kyei I, Agyemang C, Mbanya JC. Incidence and determinants of diabetes-related lower limb amputations in Ghana, 2010–2015-a retrospective cohort study. *BMC Endocr Disord*. 2019;19:1–8. doi:10.1186/s12902-019-0353-8
9. Hegde VN, Prabhu V, Rao SB, et al. Effect of laser dose and treatment schedule on excision wound healing in diabetic mice. *Photochem Photobiol*. 2011;87:1433–1441. doi:10.1111/j.1751-1097.2011.00991.x

10. Ghotaslou R, Memar MY, Alizadeh N. Classification, microbiology and treatment of diabetic foot infections. *J Wound Care*. 2018;27:434–441. doi:10.12968/jowc.2018.27.7.434
11. Ridiandries A, Tan J, Bursill CA. The role of chemokines in wound healing. *Int J Mol Sci*. 2018;19:3217. doi:10.3390/ijms19103217
12. Rahim K, Saleha S, Zhu X, et al. Bacterial contribution in chronicity of wounds. *Microb Ecol*. 2017;73:710–721. doi:10.1007/s00248-016-0867-9
13. Baltzis D, Eleftheriadou I, Veves A. Pathogenesis and treatment of impaired wound healing in diabetes mellitus: new insights. *Adv Ther*. 2014;31:817–836. doi:10.1007/s12325-014-0140-x
14. Oryan A, Alemzadeh E, Moshiri A. Role of sugar-based compounds on cutaneous wound healing: what is the evidence? *J Wound Care*. 2019;28:s13–s24. doi:10.12968/jowc.2019.28.Sup3b.S13
15. Zhou X, Li M, Xiao M, et al. ERβ accelerates diabetic wound healing by ameliorating hyperglycemia-induced persistent oxidative stress. *Front Endocrinol*. 2019;10:499. doi:10.3389/fendo.2019.00499
16. Ayuk SM, Houreld NN, Abrahamse H. Effect of 660 nm visible red light on cell proliferation and viability in diabetic models in vitro under stressed conditions. *Lasers Med Sci*. 2018;33:1085–1093. doi:10.1007/s10103-017-2432-2
17. Morikawa M, Derynck R, Miyazono K. TGF-β and the TGF-β family: context-dependent roles in cell and tissue physiology. *Cold Spring Harb Perspect Biol*. 2016;8:a021873. doi:10.1101/cshperspect.a021873
18. Zhong J, Hu N, Xiong X, Lei Q, Li L. A novel promising therapy for skin aging: dermal multipotent stem cells against photoaged skin by activation of TGF-β/Smad and p38 MAPK signaling pathway. *Med Hypotheses*. 2011;76:343–346. doi:10.1016/j.mehy.2010.10.035
19. Luo K. Signaling cross talk between TGF-β/Smad and other signaling pathways. *Cold Spring Harb Perspect Biol*. 2017;9:a022137. doi:10.1101/cshperspect.a022137
20. Barrientos S, Stojadinovic O, Golinko MS, Brem H, Tomic-Canic M. Growth factors and cytokines in wound healing. *Wound Repair Regen*. 2008;16:585–601. doi:10.1111/j.1524-475X.2008.00410.x
21. Shi Y, Massagué J. Mechanisms of TGF-β signaling from cell membrane to the nucleus. *Cell*. 2003;113:685–700. doi:10.1016/S0092-8674(03)00432-X
22. Han G, Ceilley R. Chronic wound healing: a review of current management and treatments. *Adv Ther*. 2017;34:599–610.
23. Spampinato SF, Caruso GI, De Pasquale R, Sortino MA, Merlo S. The treatment of impaired wound healing in diabetes: looking among old drugs. *Pharmaceuticals*. 2020;13:60. doi:10.3390/ph13040060
24. Houreld NN. Shedding light on a new treatment for diabetic wound healing: a review on phototherapy. *Sci. World J*. 2014;2014:1–13. doi:10.1155/2014/398412
25. Al-Watban FAH, Dai T, Hamblin MR, et al. Effect of red and near-infrared wavelengths on low-level laser (light) therapy-induced healing of partial-thickness dermal abrasion in mice. *Photomed Laser Surg*. 2014;47:72–77.
26. Houreld N, Abrahamse H. Low-intensity laser irradiation stimulates wound healing in diabetic wounded fibroblast cells (WS1). *Diabetes Technol Ther*. 2010;12:971–978. doi:10.1089/dia.2010.0039
27. Chen H, Tu M, Shi J, et al. Effect of photobiomodulation on CCC-ESF reactive oxygen species steady-state in high glucose mediums. *Lasers Med Sci*. 2021;36:555–562. doi:10.1007/s10103-020-03057-4
28. Jere SW, Houreld NN, Abrahamse H. Photobiomodulation at 660 nm stimulates proliferation and migration of diabetic wounded cells via the expression of epidermal growth factor and the JAK/STAT pathway. *J Photochem Photobiol B Biol*. 2018;179:74–83. doi:10.1016/j.jphotobiol.2017.12.026
29. Ayuk SM, Houreld NN, Abrahamse H. Effect of 660 nm visible red light on cell proliferation and viability in diabetic models in vitro under stressed conditions. *Lasers Med Sci*. 2018;33:1085–1093.
30. Oyebode O, Houreld NN, Abrahamse H. Photobiomodulation in diabetic wound healing: a review of red and near-infrared wavelength applications. *Cell Biochem Funct*. 2021;39(5):596–612. doi:10.1002/CBF.3629
31. Mokoena DR, Houreld NN, Dhilip Kumar SS, Abrahamse H. Photobiomodulation at 660 nm Stimulates Fibroblast Differentiation. *Lasers Surg Med*. 2019;52(7):671–681. doi:10.1002/lsm.23204
32. Hayes O, Ramos B, Rodriguez LL, Aguilar A, Badia T, Castro FO. Cell confluency is as efficient as serum starvation for inducing arrest in the G0/G1 phase of cell cycle in granulose and fibroblast cells of cattle. *Anim Reprod Sci*. 2005;87:181–192. doi:10.1016/j.anireprosci.2004.11.011
33. Rigau J, Sun CH, Trelles MA, Berns MW. Effects of the 633-nm laser on the behavior and morphology of primary fibroblast culture. in Effects of Low-Power Light on Biological Systems. *Int Soc Optics Photonics*. 1996;2630:38–42.
34. Chen ZJ, Yang JP, Wu BM, Tawil B. A novel three-dimensional wound healing model. *J Dev Biol*. 2014;2:198–209. doi:10.3390/jdb2040198
35. Martinotti S, Ranzato E. Scratch wound healing assay. *Epidermal Cells*. 2019;2:225–229.
36. Walter MNM, Wright KT, Fuller HR, MacNeil S, Johnson WEB. Mesenchymal stem cell-conditioned medium accelerates skin wound healing: an in vitro study of fibroblast and keratinocyte scratch assays. *Exp Cell Res*. 2010;316:1271–1281. doi:10.1016/j.yexcr.2010.02.026
37. Houreld N, Abrahamse H. Irradiation with a 632.8 nm helium-neon laser with 5 J/cm^2 stimulates proliferation and expression of interleukin-6 in diabetic wounded fibroblast cells. *Diabetes Technol Ther*. 2007;9:451–459. doi:10.1089/dia.2007.0203
38. Felice F, Zambito Y, Belardinelli E, et al. Effect of different chitosan derivatives on in vitro scratch wound assay: a comparative study. *Int J Biol Macromol*. 2015;76:236–241. doi:10.1016/j.ijbiomac.2015.02.041
39. Chaves ME. Effects of low-power light therapy on wound healing: LASER x LED. *An Bras Dermatol*. 2014;89:616–623. doi:10.1590/abd1806-4841.20142519
40. Ayuk SM, Houreld NN, Abrahamse H. Laser Irradiation Alters the Expression Profile of Genes Involved in the Extracellular Matrix In Vitro. *Int. J. Photoenergy*. 2014;2014:1–17. doi:10.1155/2014/604518
41. Zare F, Moradi A, Fallahnezhad S, et al. Photobiomodulation with 630 plus 810 nm wavelengths induce more in vitro cell viability of human adipose stem cells than human bone marrow-derived stem cells. *J Photochem Photobiol B Biol*. 2019;201:111658. doi:10.1016/j.jphotobiol.2019.111658
42. Sekhejane PR, Houreld NN, Abrahamse H. Irradiation at 636 nm positively affects diabetic wounded and hypoxic cells in vitro. *Photomed Laser Surg*. 2011;29:521–530. doi:10.1089/pho.2010.2877
43. Stadelmann WK, Digenis AG, Tobin GR. Physiology and healing dynamics of chronic cutaneous wounds. *Am J Surg*. 1998;176:26S–38S. doi:10.1016/S0002-9610(98)00183-4

44. Liu P, Choi JW, Lee MK, Choi YH, Nam TJ. Wound healing potential of spirulina protein on CCD-986sk cells. *Mar Drugs*. 2019;17:130. doi:10.3390/md17020130
45. Masson-Meyers DS, Bumah VV, Enwemeka CS. Blue light does not impair wound healing in vitro. *J Photochem Photobiol B Biol*. 2016;160:53–60. doi:10.1016/j.jphotobiol.2016.04.007
46. Simpson KJ, Selfors LM, Bui J, et al. Identification of genes that regulate epithelial cell migration using an siRNA screening approach. *Nat Cell Biol*. 2008;10:1027–1038. doi:10.1038/ncb1762
47. Chen Y. Scratch wound healing assay. *Bio-Protocol*. 2012;2:e100–e100. doi:10.21769/BioProtoc.100
48. Etemadi A, Namin ST, Hodjat M, Kosarieh E, Hakimiha N. Assessment of the Photobiomodulation Effect of a Blue Diode Laser on the Proliferation and Migration of Cultured Human Gingival Fibroblast Cells: a Preliminary In Vitro Study. *J Lasers Med Sci*. 2020;11:491. doi:10.34172/jlms.2020.77
49. Houreld N, Sekhejane PR, Abrahamse H Low intensity laser irradiation stimulates healing in stressed models 8th International Congress of World Association of Laser Therapy held in Bergen, Norway 23–26; 2010.
50. Chung T, Peplow PV, Baxter GD. Laser photobiostimulation of wound healing: defining a dose response for splinted wounds in diabetic mice. *Lasers Surg Med*. 2010;42:816–824. doi:10.1002/lsm.20981
51. Kocherova I, Bryja A, Błochowiak K, et al. Photobiomodulation with red and near-infrared light improves viability and modulates expression of mesenchymal and apoptotic-related markers in human gingival fibroblasts. *Materials*. 2021;14(12):3427. doi:10.3390/ma14123427
52. da Silva PA. Photobiomodulation can alter mRNA levels cell death-related. *Lasers Med Sci*. 2019;34:1373–1380. doi:10.1007/s10103-019-02732-5
53. Bartkova J, Grøn B, Dabelsteen E, Bartek J. Cell-cycle regulatory proteins in human wound healing. *Arch Oral Biol*. 2003;48:125–132. doi:10.1016/S0003-9969(02)00202-9
54. Bertoli C, Skotheim JM, De Bruin RAM. Control of cell cycle transcription during G1 and S phases. *Nat Rev Mol Cell Biol*. 2013;14:518–528. doi:10.1038/nrm3629
55. Li LJ, Wu F, Zhang JQ, et al. The crude ethanol extract of Periplaneta americana L. stimulates wound healing in vitro & in vivo. *Chin Med*. 2019;14:1–9. doi:10.1186/s13020-019-0259-4
56. Zahm J, Kaplan H, Herard A, et al. Cell migration and proliferation during the in vitro wound repair of the respiratory epithelium. *Cell Motil Cytoskeleton*. 1997;37:33–43. doi:10.1002/(SICI)1097-0169(1997)37:1<33::AID-CM4>3.0.CO;2-I
57. Miyazawa K, Miyazono K. Regulation of TGF-β family signaling by inhibitory Smads. *Cold Spring Harb Perspect Biol*. 2017;9:a022095. doi:10.1101/cshperspect.a022095
58. Wang XJ, Han G, Owens P, Siddiqui Y, Li AG. Role of TGFβ-mediated inflammation in cutaneous wound healing. *J Investigative Dermatol Symposium Proce*. 2006;11:112–117. doi:10.1038/sj.jidsymp.5650004
59. Chen X, Thibeault SL. Response of fibroblasts to transforming growth factor-β1 on two-dimensional and in three-dimensional hyaluronan hydrogels. *Tissue Eng Part A*. 2012;18:2528–2538. doi:10.1089/ten.tea.2012.0094
60. Branton MH, Kopp JB. TGF-β and fibrosis. *Microbes Infect*. 1999;1:1349–1365. doi:10.1016/S1286-4579(99)00250-6
61. Border WA, Noble NA. Transforming growth factor β in tissue fibrosis. *N Engl J Med*. 1994;331:1286–1292. doi:10.1056/NEJM199411103311907
62. Krummel TM, Michna BA, Thomas BL, et al. Transforming growth factor beta (TGF-β) induces fibrosis in a fetal wound model. *J Pediatr Surg*. 1988;23:647–652. doi:10.1016/S0022-3468(88)80638-9
63. Vyas B, Ishikawa K, Duflo S, Chen X, Thibeault S. Inhibitory effects of HGF and IL-6 on TGF-β1 mediated vocal fibroblast-myofibroblast differentiation. *Ann Otol Rhinol Laryngol*. 2010;119:350. doi:10.1177/000348941011900513
64. Klass BR, Grobbelaar AO, Rolfe KJ. Transforming growth factor β1 signalling, wound healing and repair: a multifunctional cytokine with clinical implications for wound repair, a delicate balance. *Postgrad Med J*. 2009;85:9–14. doi:10.1136/pgmj.2008.069831
65. Mauviel A. Transforming growth factor-β signaling in skin: stromal to epithelial cross-talk. *J Invest Dermatol*. 2009;129:7–9. doi:10.1038/jid.2008.385
66. Viloria-Petit A, Richard A, Zours S, Jarad M, Coomber BL. Role of transforming growth factor beta in angiogenesis. *Biochemical Basis Therapeutic Implications Angiogenesis*. 2013;2;23–45.
67. Xu X, Zhao Z, Huang Z, et al. Transforming growth factor-β in stem cells and tissue homeostasis. *Bone Res*. 2018;6:1–31. doi:10.1038/s41413-017-0004-5
68. Zhang YE. Non-Smad pathways in TGF-β signaling. *Cell Res*. 2009;19:128–139. doi:10.1038/cr.2008.328